SSSU 113
ISSN 0140 3818

UNIVERSITY OF SOUTHAMPTON

DEPARTMENT OF SHIP SCIENCE

FACULTY OF ENGINEERING

AND APPLIED SCIENCE

THEORETICAL PREDICTION OF THE SEAKEEPING CHARACTERISTICS OF TWO FAST DISPLACEMENT CATAMARANS IN OBLIQUE SEAS

J.F. Wellicome, P. Temarel, A.F. Molland & D.A. Hudson

Ship Science Report 113

March 1999

Ship Science Report No. 113/99
Theoretical Prediction of the Seakeeping Characteristics of Two Fast Displacement Catamarans in Oblique Seas

Dr J.F. Wellicome, Dr P. Temarel, Dr A.F. Molland and Mr D.A. Hudson

March 1999

Abstract

This report employs two different three-dimensional potential flow analyses to evaluate the hydrodynamic coefficients and responses of two high speed displacement catamaran forms. The hullforms are based on the NPL round-bilge series and the Series 64 form. For each hullform two catamaran demihull spacings are considered. These configurations are investigated in regular deep water waves at three different heading angles; namely head seas ($\chi = 180°$), $\chi = 150°$ and $\chi = 120°$, and for a forward speed corresponding to a Froude number of 0.65.

A selection of hydrodynamic coefficients are presented, together with heave, pitch and roll responses for all of the configurations examined. Comparisons with experimental measurements are included and discussed. Differences between the two three-dimensional methods are discussed and the limitations of the current theoretical methods highlighted. Possible ways to improve the theoretical models are outlined with particular reference to:

a) The treatment of forward speed effects,

b) Viscous damping effects around the resonant frequencies,

c) The effects of changes in hull attitude with forward speed,

d) The modelling of a transom stern, particularly at high forward speeds.

Contents

List of Tables

List of Figures

1 Introduction

The last decade has seen a considerable increase in the number of high speed craft operating throughout the world. This has led to a corresponding increase in the need to understand, and be able to predict, all aspects of the behaviour of such vessels both in calm water and in waves. The subsequent research has focused both on experimental and theoretical approaches to these problems.

Initially work was directed towards investigation of the calm water characteristics of catamarans and this has been investigated in detail at the University of Southampton over a number of years (e.g. Molland et al. (1996)). Subsequently research has investigated the performance of high speed catamarans in regular head waves, both experimentally (e.g. Wellicome et al. (1995a)) and using theoretical techniques (e.g. Wellicome et al. (1995b)). Most recently the performance of these vessels has been studied experimentally in regular and irregular oblique seas (Wellicome et al. (1999)). This report contains the results of the theoretical prediction of the seakeeping characteristics of two high speed displacement catamaran hullforms, each with two different configurations, in regular oblique waves. Theoretical approaches of differing complexity were used and predictions were compared with experimental measurements. The advantages and disadvantages associated with each method are discussed.

2 Model Details

The theoretical investigation was undertaken using the same hullforms as were used in the experimental study in oblique waves. Namely, using the notation of Wellicome et al. (1999), a catamaran based on the NPL round bilge series designated as model 5b and a catamaran based on the Series 64 form designated as model 5s. Principal particulars of the models are given in table 1. Where there are differences between the design and tested conditions; the design condition was used for calculations throughout. The two catamarans are of equal length and displacement, but differ significantly in their underwater hull form. Both models are of symmetrical round bilge form with a transom stern. Body plans are presented in figure 1. These hullforms are broadly representative of a number of catamarans in service.

For details of the construction of the models used in the experimental work reference should be made to Wellicome et al. (1999).

Each of the catamaran forms was investigated in two configurations; with centreline to centreline separation to length (S/L) ratios of 0.2 and 0.4. Theoretical predictions were made for each of these configurations at a Froude number (Fn) of 0.65 and for regular waves of heading angle (χ) between the wave direction and course angle of 180°, 150° and 120°; 180° being head seas (Wellicome et al. (1999)).

The centre of gravity was positioned coincident with the LCB in the longitudinal direction and as measured on the experimental model in the vertical direction. The moments of inertia in roll, pitch and yaw were also taken from the experimental model arrangement. These are summarised in table 2.

3 Mathematical Model

It is not the intention of the present report to repeat a full derivation of the boundary value problem for a surface piercing body travelling with forward speed as this has been done at length in many places, see, for example Bishop et al. (1986).

3.1 Equations of Motion

The motions of a rigid vessel undergoing small perturbations, in regular sinusoidal waves, about an equilibrium axis system $0xyz$ situated in the calm water surface vertically above or below the centre of gravity can be represented by the coupled linear equations of motion:

$$\sum_{k=1}^{6} \left\{ -\omega_e^2 \left(M_{jk} + A_{jk} \right) + i\omega_e B_{jk} + C_{jk} \right\} \eta_k = F_j \quad \text{for } j = 1, 2, \ldots, 6, \tag{1}$$

where,
η_k is the complex motion amplitude,
ω_e is frequency of encounter,
C_{jk} is an element of the hydrostatic restoring matrix,
A_{jk} is the added mass in the jth mode due to unit motion in the kth direction,
B_{jk} is the damping coefficient in the jth mode due to unit motion in the kth direction,
F_j is the complex amplitude of the wave exciting force,
M_{jk} is an element of the generalised mass matrix, which for a body with lateral symmetry may be written,

$$M_{jk} = \begin{bmatrix} M & 0 & 0 & 0 & Mz_G & 0 \\ 0 & M & 0 & -Mz_G & 0 & 0 \\ 0 & 0 & M & 0 & 0 & 0 \\ 0 & -Mz_G & 0 & I_{44} & 0 & -I_{46} \\ Mz_G & 0 & 0 & 0 & I_{55} & 0 \\ 0 & 0 & 0 & -I_{46} & 0 & I_{66} \end{bmatrix} \tag{2}$$

where, M is the mass of the vessel, I_{jj} is the moment of inertia in the jth mode of motion about the centre of gravity G situated at $(0, 0, z_G)$ and I_{jk} is the cross-product of inertia. For a body with lateral symmetry the only non-zero elements in the hydrostatic restoring matrix are $C_{33}, C_{35} = C_{53}, C_{44}$ and C_{55}.

The terms in equation 1 can be evaluated by a number of methods; such as two-dimensional strip theory and three-dimensional potential flow analysis, each assuming the fluid inviscid, incompressible and the fluid motion irrotational (e.g. Salvesen et al. (1970), Inglis and Price (1982a)). The fluid motion can be represented by a velocity potential function satisfying Laplace's equation throughout the fluid domain. Unfortunately calculating the total velocity potential in its most general form is difficult and, for practical use, some simplification is necessary. Thus, the total potential can be expressed as a linear summation of components,

$$\phi(x, y, z, y) = (Ux + \phi_s(x, y, z)) + \phi_T e^{i\omega_e t}, \tag{3}$$

where,

U is the forward speed,
ϕ_s is the perturbation potential due to steady translation and
ϕ_T is the unsteady perturbation potential which may be decomposed to give:

$$\phi_T = \phi_I + \phi_D + \sum_{j=1}^{6} \phi_j \eta_j, \tag{4}$$

with

ϕ_I as the incident wave potential,
ϕ_D as the diffraction potential and
ϕ_j denoting the radiation potential due to unit motion in the jth direction.

In equation 3 the first two terms represent the problem of the ship advancing at steady forward speed in calm water. These may be determined separately from the unsteady potentials. Using equation 4 and appropriate boundary conditions solutions to equations 1 are obtained.

3.2 Methods of Evaluation

Evaluation of the radiation and diffraction potentials in equation 4, which are used to calculate the added mass and damping coefficients and the diffraction component of the wave exciting force respectively, may be carried out in several different ways (Newman (1978)). For this study, two alternative three-dimensional methods were used.

The three-dimensional analysis is a boundary element method, whereby the problem of modelling the whole fluid domain can be reduced to that of modelling the boundaries of the fluid, in this case by application of Green's 2nd theorem. By suitable choice of the singularity to be used, the problem can be further reduced to modelling the body surface only. Thus, in the three-dimensional method adopted the wetted surface of the hull is represented by four-cornered panels, each of which contains a singularity at its centre. For the NPL model 5b 640 panels were used to represent the wetted hull surface (320 per demihull) and for the Series 64 model 5s, 700 panels (350 per demihull) were distributed over the wetted surface. These representations of the wetted surface are illustrated in figure 2.

In this study two types of singularity were used, a pulsating source (Bishop et al. (1986)) and a translating pulsating source (Inglis and Price (1982a), Inglis and Price (1982b)). Both of these singularities satisfy the Laplace equation throughout the fluid domain, a radiation condition at infinity and a linearised free surface condition. The difference between the two three-dimensional methods is in the application of this linear free surface boundary condition. The pulsating source potential satisfies a further simplification assuming low forward speed and high frequencies of oscillation. Thus, whilst the translating pulsating source distribution inherently includes the effects of forward speed through the full linearised free surface boundary condition the pulsating source distribution accounts for forward speed in a limited manner through corrections to the zero speed solution in a similar manner to strip theory (Inglis and Price (1981b)).

Neither distribution includes interaction effects between the steady and unsteady components of the velocity potential. This arises from the assumption, when formulating the boundary condition on the hull surface, that the perturbation of the steady flow due to the presence of the hull is negligible. This assumption is physically justifiable when slender ships are being considered (Inglis and Price (1981b)).

Since the earlier application of the translating pulsating source distribution for the NPL model 4b in head seas (Wellicome et al. (1995b)), the method has undergone extensive verification and validation with an alternative theoretical model satisfying the same boundary conditions, together with experimental data. For the validation exercise predictions using the formulation of the translating pulsating source potential given by Inglis and Price (1981a) were compared with those obtained using an alternative formulation given by Du and Wu (1998). This investigation was undertaken for source-field point characteristics, an ellipsoid travelling in regular waves (Du et al. (1999b)) and subsequently for the Series 60 hull form, a NPL mono-hull form (Du et al. (1999a)) and an idealised multi-hull form (Bailey et al. (1998a)) travelling in regular waves. In the course of these investigations great care was taken to validate intermediate steps in the calculation, as well as to compare the computational effort associated with either method.

These studies show the remarkable agreement in the numerically derived data from the two separate mathematical formulations and numerical schemes of study over wide ranges of speed and frequency. Additionally, comparisons between the two methods, experimental data and predictions obtained by the pulsating source method indicate the importance of using a method that inherently accounts for the influence of forward speed in the solution, even for the relatively low speeds considered for a Series 60 hull form (Bailey et al. (1998b)). This is especially true for antisymmetric modes of motion.

This validation exercise has resulted in numerical improvements and confidence that the translating pulsating source method is suitable for the analysis of catamaran vessels travelling with high forward speed at any frequency of encounter.

4 Results

4.1 Hydrodynamic Coefficients

The hydrodynamic coefficients related to the heave added mass and damping are presented for the Series 64 model 5s, at both separations, in figures 3 and 5. The roll added mass and damping are presented in figures 4 and 6.

As has been discussed previously (Hudson et al. (1995)), the added mass for a multihull differs from that of a monohull in any mode of motion in that in certain regions it exhibits troughs which may result in negative values, particularly at low Froude numbers. These troughs are caused by the fluid interaction between the hulls. For symmetric modes of motions (i.e. heave and pitch) this interaction may take the form of a vertical oscillation of the fluid trapped between the hulls, or of a symmetric standing wave formed between the hulls. For antisymmetric modes of motion (i.e. sway, roll and yaw) the interaction is always of a standing wave form. As may be expected the fluid interaction is a function of both the forward speed and the distance between the hulls.

Predictions obtained by the pulsating source distribution illustrate these different interactions. Thus, the first trough in the added mass curves, at $\delta = \omega_e\sqrt{L/g} \approx 3.25$ for S/L=0.2 (Fig. 5) and at $\delta \approx 2.5$ for S/L=0.4 (Fig. 3) may be associated with the first type of symmetric interaction. Similarly the apparent discontinuity in the added mass curve for S/L=0.4, seen at $\delta \approx 4.4$ is associated with the second form of symmetric interaction, that of a symmetric standing wave. The discontinuities in the roll added mass curves, at $\delta \approx 5.1$ for S/L=0.2 (Fig. 6) and at $\delta \approx 3.5$ for S/L=0.4 (Fig. 4) may be identified with the formation of an antisymmetric standing wave between the hulls. The frequency at which these standing waves will occur can be accurately predicted by the usual deep water gravity wave equation. With any form of interaction the damping curves exhibit a peak in the region where the added mass has its maximum slope and vice versa.

These fluid interactions are not visible in the predictions obtained using the translating pulsating source method at the speed considered (Fn=0.65). When the speed is gradually reduced to zero, predictions using the translating pulsating source method indicate increasing interaction between the hulls, until at zero speed predictions agree with the pulsating source method (Bailey et al. (1998a)). This confirms that the fluid/structure interaction is a function of the forward speed of the vessel.

4.2 Responses

Heave, pitch and roll responses for all of the vessel configurations and wave headings are presented in figures 7 to 22. Responses are presented in the form of heave transfer function (TF)=heave amplitude/wave amplitude (a), pitch transfer function=pitch amplitude/equivalent wave slope (ka) and roll transfer function=roll amplitude/equivalent wave slope (ka). These responses are plotted as functions of non-dimensional frequency of encounter, $\delta = \omega_e\sqrt{L/g}$. Experimental data taken from Wellicome et al. (1999) is plotted on the graphs.

4.2.1 Model 5b

From figures 7 to 9 for Model 5b at S/L=0.4 it is evident that the heave and pitch responses predicted by the pulsating source method exhibit two peaks for all of the three wave headings ($\chi = 180°, 150°$ and 120°). Both the experimental results and those obtained using the translating pulsating source method exhibit only one peak. The second of the two peaks can be associated with the troughs seen in the added mass curves for this vessel and may thus be attributed to the formation of a symmetric standing wave between the hulls. As the translating pulsating source method does not predict these troughs in the added mass curve the corresponding peak is also eliminated.

Comparing the theoretical predictions of response with the experimental data the magnitude of the resonant heave response is over-estimated by the translating pulsating source model for $\chi = 180°$

and $\chi = 150°$, but accurately predicted for $\chi = 120°$. The predicted resonant frequency higher than the experimental data in all cases. The magnitude of the first peak in the pulsating source predictions also agrees well with the experimental data; in this case being lower for $\chi = 180°$ and $\chi = 150°$ but higher for $\chi = 120°$. The second peak is not present in the experimental data available. For $\chi = 180°$ and $\chi = 150°$ the translating pulsating source model over-predicts the resonant pitch response and once again the resonant frequency is also higher. The first peak in the pulsating source predictions again agrees well with the experimental data at these headings, but there is no second peak in the experimental results. At $\chi = 120°$ both methods agree well with the experimental data, predictions by the translating pulsating source method being, overall, more accurate.

In the case of the roll response the translating pulsating source predictions agree well with the experimental data at all frequencies and for both $\chi = 150°$ and $\chi = 120°$ (Fig. 10). Predictions obtained by the pulsating source model exhibit two peaks, neither of which is evident in the experimental results. These may be associated with the troughs seen in the added mass curve and can thus be attributed to the formation of the first and second harmonic antisymmetric standing wave respectively.

When the separation is reduced to S/L=0.2, the translating pulsating source method predicts the heave response accurately at $\chi = 180°$ and $\chi = 150°$ both in terms of the magnitude of the response and the frequency of resonance. At $\chi = 120°$ the frequency of resonance is accurately predicted, but the magnitude of the response is under-estimated. The pulsating source method over-predicts the resonant response in terms of magnitude and frequency at all headings. As a consequence of the narrower separation between the hulls the frequency at which symmetric standing wave effects are seen in the pulsating source predictions is outside the range of frequencies for which results are presented in figures 11 and 12. Both methods over-predict the pitch response at all headings.

The roll response predicted by the theoretical methods exhibits the correct trends at either heading, but the magnitude of the resonant response is over-predicted, as is the frequency. The pulsating source method again predicts a second peak not seen in the experimental results which may be attributed to the first antisymmetric standing wave between the hulls.

In order to more clearly illustrate the manner in which the response of the vessel varies with wave heading experimental data and predictions by the translating pulsating source model are shown for all three headings in figures 23 to 28 for Model 5b, S/L=0.4 and S/L=0.2. For S/L=0.4, the variation in response with wave heading is accurately predicted by this theoretical model for heave, pitch and roll. The magnitude of the response is accurately predicted for heave and roll; but pitch is over-predicted. This is again true for S/L=0.2. For S/L=0.2, experimental data indicate the heave response reduces less moving from $\chi = 150°$ to $\chi = 120°$ than for S/L=0.4. This is reflected in the theoretical predictions.

4.2.2 Model 5s

Responses of the Series 64 model 5s are illustrated in figures 15 to 22. For S/L=0.4 and $\chi = 180°$ and $\chi = 150°$ the resonant heave magnitude is accurately predicted by the translating pulsating source method. The resonant frequency is higher. The first peak predicted by the pulsating source method appears at the right frequency for resonance, but the corresponding magnitude of the response is too low. The remaining two peaks predicted by this method, which can be attributed to the formation of symmetric standing waves between the hulls, are not seen in the experimental data as per model 5b. However, it should be noted that the magnitude of the second peak agrees well with the experimental data although it occurs at a frequency that is higher than the translating pulsating source predictions and the experimental data. For $\chi = 120°$ the translating pulsating source under-predicts the peak in the experimental results. The first peak of the pulsating source method predictions is in better agreement.

As with model 5b, for $\chi = 180°$ and $\chi = 150°$ the pitch response is over-estimated by the translating pulsating source model. The first peak in the pulsating source results is in good agreement with the

experimental data. For $\chi = 120°$ the translating pulsating source results agree, overall, closely.

Unlike model 5b experimental data for the roll response of model 5s, S/L=0.4 exhibits a notable resonance peak. This is not predicted to the same extent by the translating pulsating source model. The pulsating source method does indicate a resonant response but this is at a higher frequency and is larger in magnitude. This predicted resonant response and subsequent peaks can again be attributed to the formation of an antisymmetric standing wave between the hulls.

For S/L=0.2, the magnitude of the heave resonance peak is over-predicted by the translating pulsating source model, although the frequency at which this resonance occurs is well predicted. This is true for all three wave headings. The pulsating source model over-predicts the magnitude and frequency of the resonant peak significantly for all wave headings. Both methods over-predict pitch response at all headings. The translating pulsating source method gives better predictions of the resonant frequency.

Roll response is over-predicted at resonance by either method but the position of the resonance frequency is accurately predicted. The effect of the first antisymmetric standing wave can also be seen in the pulsating source predictions as a second peak.

As for model 5b, the trends with wave heading are illustrated in figures 29 to 34 for the experimental data and the translating pulsating source method. For S/L=0.4 the trends as wave heading changes are well predicted by this theoretical method for heave, pitch and roll. Magnitudes are accurate in heave, and to a lesser extent, roll. For S/L=0.2, trends with wave heading are again well predicted by the translating pulsating source model. Magnitudes are again accurate in heave. The reduction in heave response between $\chi = 150°$ and $\chi = 120°$ is again less for S/L=0.2 as compared to S/L=0.4. This is seen in both the experimental measurements and the theoretical predictions.

4.3 Discussion

From the results presented it is evident that for the pulsating source distribution method there are two main discrepancies between the theoretical and experimental results. The first of these is the existence of secondary (resonant) peaks in the heave, pitch and roll response characteristics for the wider separation of S/L=0.4 and, for roll only, when S/L=0.2 within the range of frequencies investigated. These secondary peaks are due to the existence of standing waves between the hulls and are not present in the experimental results. The reason for their existence in the pulsating source method predictions is the inadequate treatment of forward speed in this formulation. Solving the zero forward speed free surface boundary condition essentially means that interaction between the hulls of the catamaran takes place at the same longitudinal section; whereas in reality the region of interaction is reduced with forward speed. Increases in separation also reduce the region of interaction when the vessel has forward speed. A two-dimensional strip theory approach suffers from the same problem as the pulsating source distribution method, as was discussed in the previous work into head sea responses (Wellicome et al. (1995b)). If interaction between the hulls of the catamaran were simply ignored then the pulsating source distribution technique may give more satisfactory predictions, both in terms of trends and magnitudes of response. Unfortunately such an assumption requires *a priori* judgements to be made concerning the speed and separation of the catamaran and the method loses its flexibility.

The translating pulsating source distribution method eliminates these secondary peaks in response caused by standing waves between the hulls since it satisfies the free surface boundary condition with forward speed.

The second main discrepancy between theory and experiment with the pulsating source method is the over-prediction of resonant heave and pitch responses for model 5b, S/L=0.2 and model 5s, S/L=0.2. For this narrow separation the prediction of resonant frequencies is less accurate. In general the first resonant peaks predicted by the pulsating source distribution technique for model 5b, S/L=0.4 are in good agreement with the experimental data. This is also true for model 5s.

The translating pulsating source method gives good qualitative results for both hull forms at both separations for all motions; and the magnitude of the heave response is generally well predicted throughout. The main discrepancy between theoretical predictions and experimental data for this method is the over-prediction of pitch response. This is true for both models at either separation; certainly for $\chi = 180°$ and $\chi = 150°$.

Without experimental data for hydrodynamic coefficients and wave exciting forces it is difficult to ascertain the cause of this discrepancy. It may be possible that the potential flow assumptions adopted in the method lead to an under-estimation of damping, to which the results are especially sensitive around resonance. Whilst it is possible to adopt various empirically based approaches to account for viscous damping effects (see, for example Lee and Curphey (1977) and Chan (1995)) it is by no means certain that this is the physical cause of the discrepancy seen in prediction of pitch responses. The agreement of the heave response predictions, and in some cases roll response response predictions, suggest viscous damping effects may not be vitally important overall.

Considering the physical problem it is apparent that the theoretical treatment of the fluid structure interaction by the translating pulsating source method is deficient in a number of ways. The first of these is the neglection of the effects of the steady-state wave potential in the formulation of the unsteady body boundary conditions, and hence the unsteady wave potentials. Whilst this effect is generally considered small for slender ships (see, Inglis and Price (1981b)) it may be more important in the catamaran configuration where the steady waves generated by one hull will interact with those generated by the other. In order to include this interaction in an approximate manner, the body boundary conditions must be modified to allow for the steady-state wave effect, this is then solved for prior to finding the unsteady solution. It is possible to modify the translating pulsating source method to achieve this (Inglis and Price (1982a), Inglis and Price (1982b)). To be mathematically consistent the free-surface boundary condition should also be modified to account for the influence of the steady-state wave system in the unsteady problem. If this is done there is, at present, no fundamental singularity which satisfies the resulting non-linear boundary condition on the free surface. By recourse to a low-speed series approximation to this problem a solution may be found (Wu and Eatock-Taylor (1990)), but this is obviously not valid for high speeds.

Another deficiency in the theoretical method is that the fluid forces are evaluated on the mean wetted surface of the hull at rest, rather than the instantaneous running wetted surface. There are several consequences of this; the above water shape of the hull can have no influence on its motions, the effects of sinkage and trim as the vessel travels, particularly with increasing forward speed, are neglected and the transom stern running "dry" at higher Froude numbers is not modelled. Accounting for the above water shape of the hull requires a time-domain analysis of the problem, with calculation of the fluid forces at each time step on the instantaneous wetted surface of the hull. This may be undertaken by one of several methods (e.g. Lin and Yue (1990), Sclavounos et al. (1993)) which may, or may not, be fully non-linear.

The steady-state sinkage and trim of the vessel may be accounted for, even in the present methods, by adjusting the wetted surface of the hull to be the mean *running* wetted surface, rather than the mean *static* wetted surface. Unfortunately, the presence of a transom stern, running dry at the higher speeds, complicates the adoption of such a procedure in the present work. A proper treatment of the transom stern requires the inclusion of a Kutta-type condition at the stern to ensure that the pressure at this section is atmospheric.

5 Conclusions

Analytical predictions of the responses of two catamaran forms, in two configurations travelling in head and oblique waves at a Froude number of 0.65 have been carried out using two different three-dimensional methods with singularity distributions over the mean calm water wetted surface of the hull and the results compared with experimental data.

The results obtained indicate that, overall, the more complex three-dimensional analysis, namely a translating pulsating source distribution method gives more accurate agreement with the experimental data. The pulsating source distribution method suffers from an inadequate representation of the dynamic characteristics of the fluid structure interaction at high forward speeds.

Both qualitative and quantitative agreement is seen between predictions of the heave response of the catamarans using the translating pulsating source distribution method and experimental data.

Predicted roll responses are in qualitative agreement with experimental data, with some quantitative agreement also evident.

Predictions of pitch response are in general larger than the experimental data suggests. To improve the pitch response predictions for the catamarans it is clear that the translating pulsating source model requires further development. Whilst incorporating the interaction effects between the steady and unsteady wave systems, and performing the analysis about the mean running waterline are expected to provide small improvements, accounting for the above water shape of the hull as it oscillates is expected to prove most beneficial. Additional improvements are also expected with a more complete treatment of the transom stern running dry at high speeds.

The translating pulsating source distribution method reproduces the trends seen in the experimental data, both as wave heading is altered and as hull separation is increased. The ability of this method to correctly predict these trends is particularly encouraging.

Acknowledgements

The work described in this report covers part of the Fast Craft Research Programme funded by EPSRC and industry and managed by Marinetech South Ltd.

References

Bailey, P., Hudson, D., Price, W., and Temarel, P. (1998a). Theoretical validation of the hydrodynamics of high speed mono- and multi- hull vessels travelling in a seaway. In Oosterveld, M. and Tan, S., editors, *PRADS '98: The Seventh International Symposium on Practical Design of Ships and Mobile Units*, pages 567–576, The Hague, The Netherlands. Elsevier Science, B.V.

Bailey, P., Hudson, D., Price, W., and Temarel, P. (1998b). A validation of speed and frequency dependence in seakeeping. In *2nd International Shipbuilding Conference: ISC '98*, St Petersburg.

Bishop, R. E. D., Price, W. G., and Wu, Y. S. (1986). A general linear hydroelasticity theory of floating structures moving in a seaway. *Philosophical Transactions of the Royal Society*, Series A, 316:375–426.

Chan, H. (1995). On the calculations of ship motions and wave loads of high-speed catamarans. *International Shipbuilding Progress*, 42(431):181–195.

Du, S. X., Hudson, D. A., Price, W., and Temarel, P. (1999a). A theoretical validation of speed and frequency dependence in seakeeping. *Submitted for publication.*

Du, S. X., Hudson, D. A., Price, W. G., and Temarel, P. (1999b). Comparison of numerical evaluation techniques for the hydrodynamic analysis of a ship travelling in waves. *Trans. RINA*, 141.

Du, S. X. and Wu, Y. S. (1998). A fast evaluation method of the Bessho form translating and pulsating Green's function. *Shipbuilding of China*, 141(2).

Hudson, D. A., Temarel, P., and Price, W. G. (1995). Seakeeping of high speed displacement craft. In *FAST '95: Proceedings of the Third International Conference on Fast Sea Transportation*, volume 2, pages 877–892, Lübeck-Travemünde, Germany.

Inglis, R. B. and Price, W. G. (1981a). Calculation of the velocity potential of a translating, pulsating source. *Trans. RINA*, 123:163–175.

Inglis, R. B. and Price, W. G. (1981b). The influence of speed dependent boundary conditions in three dimensional ship motion problems. *International Shipbuilding Progress*, 28(318):22–29.

Inglis, R. B. and Price, W. G. (1982a). A three-dimensional ship motion theory: Calculation of wave loading and response with forward speed. *Trans. RINA*, 124:183–192.

Inglis, R. B. and Price, W. G. (1982b). A three-dimensional ship motion theory: Comparison between theoretical predictions and experimental data of the hydrodynamic coefficients with forward speed. *Trans. RINA*, 124:141–157.

Lee, C. M. and Curphey, R. M. (1977). Prediction of motion, stability and wave load of small-waterplane-area, twin hull ships. *Trans. SNAME*, 85:94–130.

Lin, W. M. and Yue, D. (1990). Numerical solutions for large amplitude ship motions in the time domain. In *18th Symposium on Naval Hydrodynamics*, pages 41–66, University of Michigan, Ann Arbor.

Molland, A. F., Wellicome, J. F., and Couser, P. (1996). Resistance experiments on a systematic series of high speed displacement catamaran forms: Variation of length-displacement ratio and breadth-draft ratio. *Trans. RINA*, 137:55–71.

Newman, J. N. (1978). The theory of ship motions. *Advances in Applied Mechanics*, 18:221–283.

Salvesen, N., Tuck, E. O., and Faltinsen, O. M. (1970). Ship motions and sea loads. *Trans. SNAME*, 78:250–280.

Sclavounos, P. D., Nakos, D. E., and Huang, Y. (1993). Seakeeping and wave induced loads on ships with flare by a Rankine panel method. In *6th Intl. Conference on Numerical Ship Hydrodynamics*, pages 57–77.

Wellicome, J., Temarel, P., Molland, A., Cic, J., and Taunton, D. (1999). Experimental measurements of the seakeeping characteristics of fast displacement catamarans in oblique waves. Ship Science Report 111/99, University of Southampton.

Wellicome, J., Temarel, P., Molland, A., and Couser, P. (1995a). Experimental measurements of the seakeeping characteristics of two fast displacement catamarans in long-crested head-seas. Ship Science Report 89, University of Southampton.

Wellicome, J., Temarel, P., Molland, A., and Hudson, D. (1995b). Theoretical prediction of the seakeeping characteristics of fast displacement catamarans. Ship Science Report 93, University of Southampton.

Wu, G. and Eatock-Taylor, R. (1990). The hydrodynamic force on an oscillating ship with low forward speed. *Journal of Fluid Mechanics*, 211:333–353.

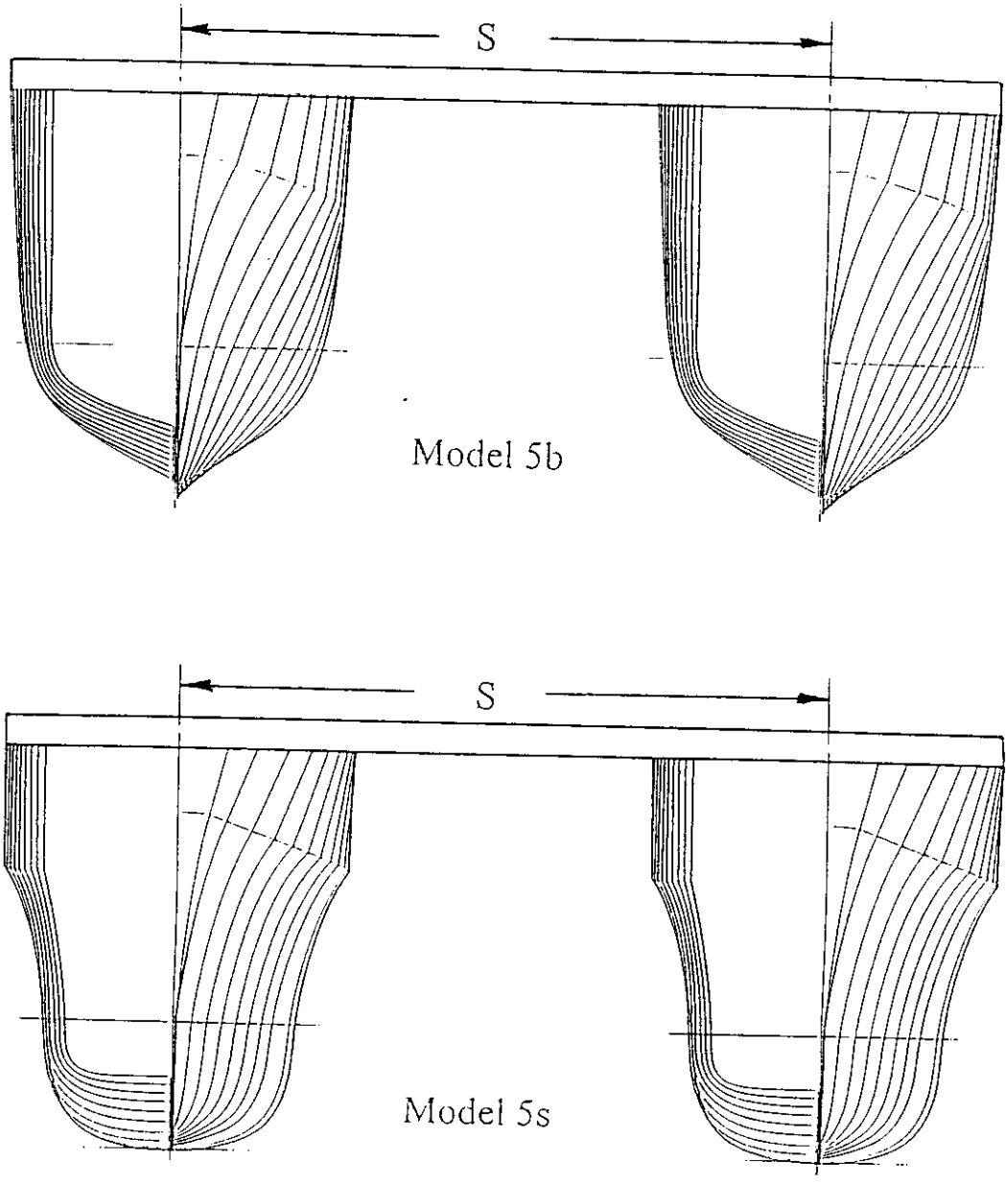

Figure 1: Body Plans for model 5b and model 5s.

Table 1: Principal particulars of models 5b and 5s (demihulls).

Model:	5b (design)	5s (design)	5b (as tested)	5s (as tested)
L (at waterline)	4.5	4.5	4.5	4.5
L/B	11.0	12.8	11.0	12.8
B/T	2.0	2.0	1.9	1.9
$L/\nabla^{1/3}$	8.5	8.5	8.3	8.3
C_B	0.397	0.537	0.400	0.540
C_p	0.693	0.633	0.698	0.637
C_m	0.573	0.848	0.573	0.848
A/L^2	0.1078	0.1095	0.1131	0.1149
LCB (% aft mid.)	6.4	6.4	6.4	6.4

Table 2: Radii of inertia for models 5b and 5s (catamaran configuration).

S/L	Pitch, k_{55}	Yaw, k_{66}	Roll, k_{44}
0.2	0.26L	0.28L	0.11L
0.4	0.26L	0.32L	0.20L

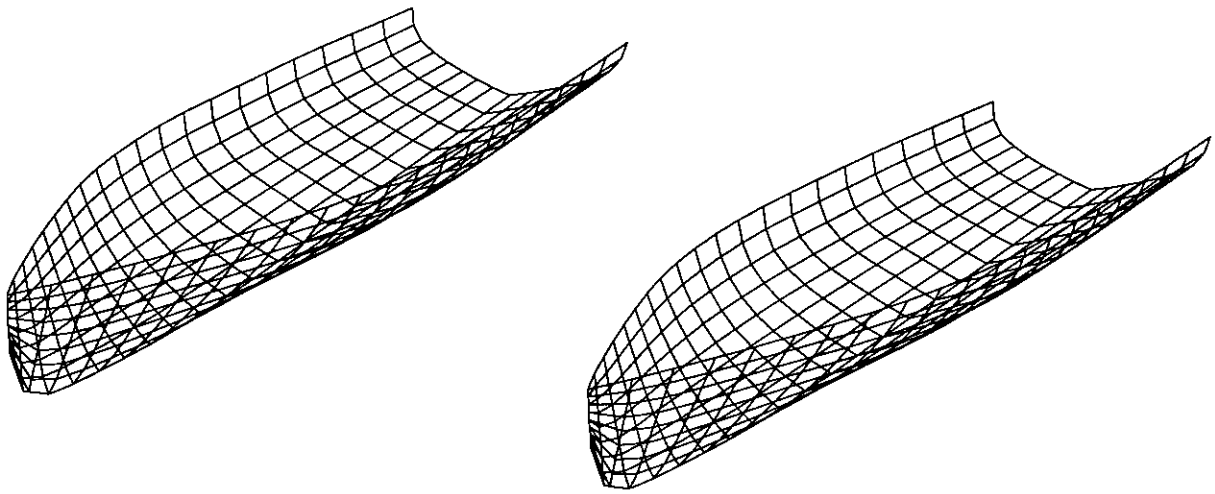

(a) model 5b, S/L=0.2, 640 panels.

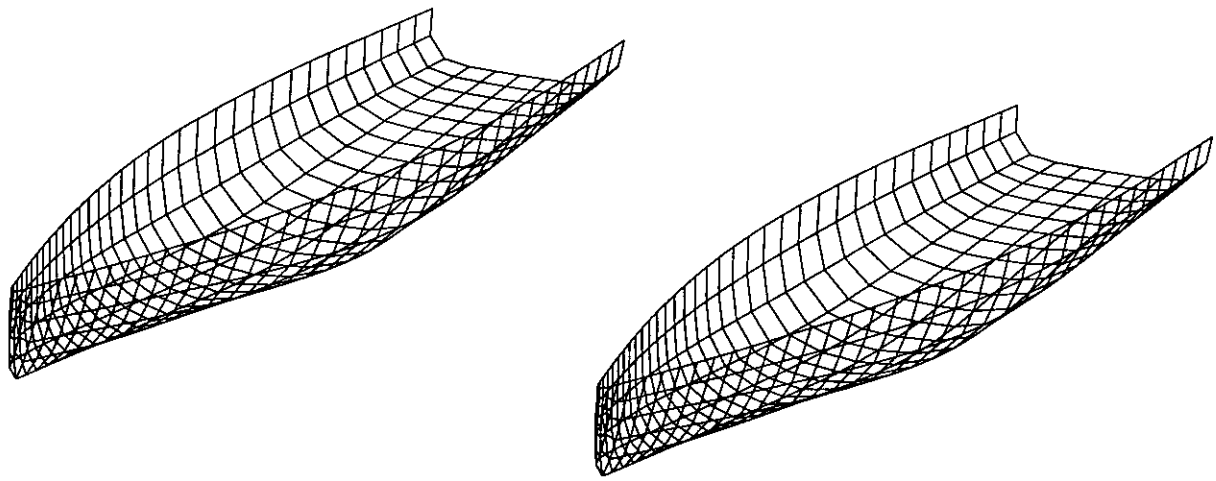

(b) model 5s, S/L=0.2, 700 panels.

Figure 2: Hull wetted surface idealisations for (a) model 5b, S/L=0.2 (640 panels) and (b) model 5s, S/L=0.20 (700 panels).

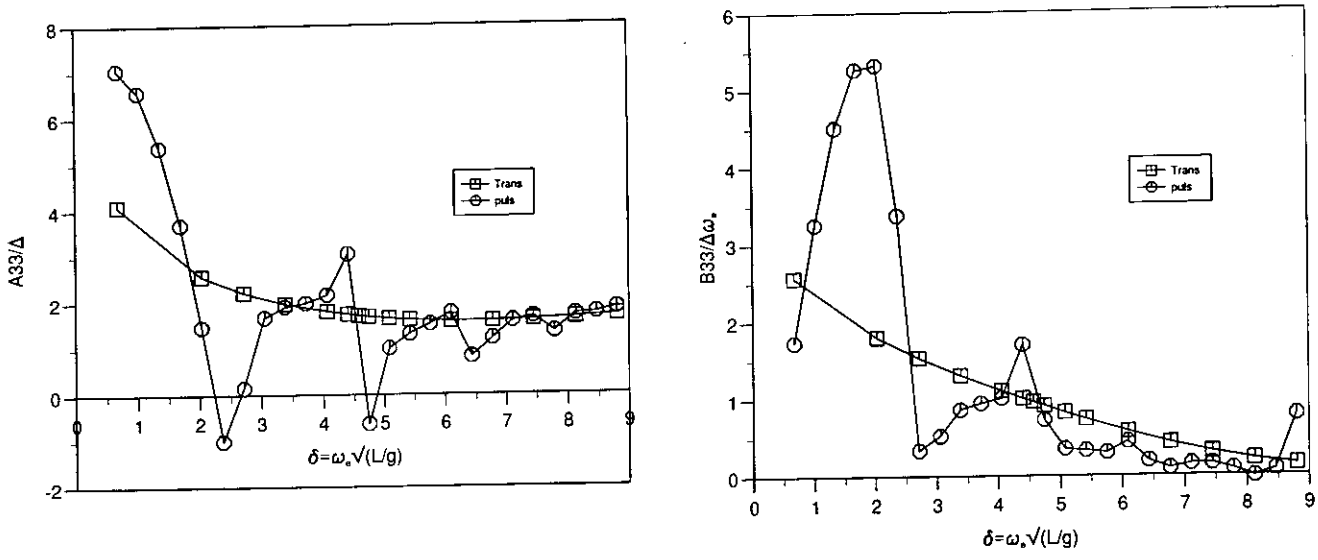

Figure 3: Heave added mass and damping coefficients for model 5s, S/L=0.4, Fn=0.65.

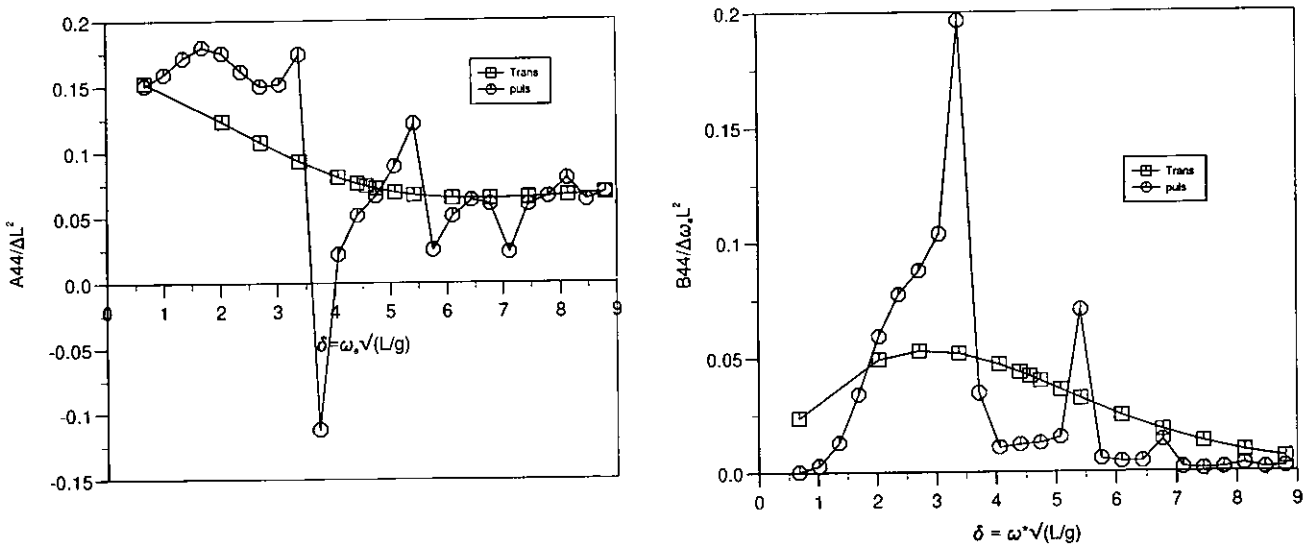

Figure 4: Roll added mass and damping coefficients for model 5s, S/L=0.4, Fn=0.65.

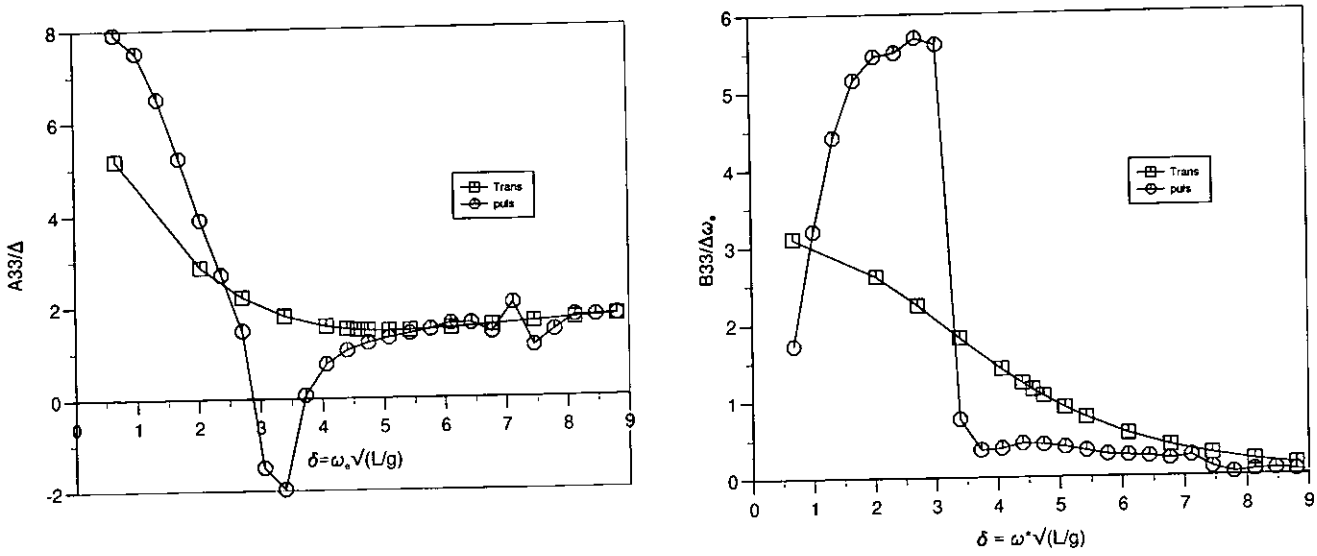

Figure 5: Heave added mass and damping coefficients for model 5s, S/L=0.2, Fn=0.65.

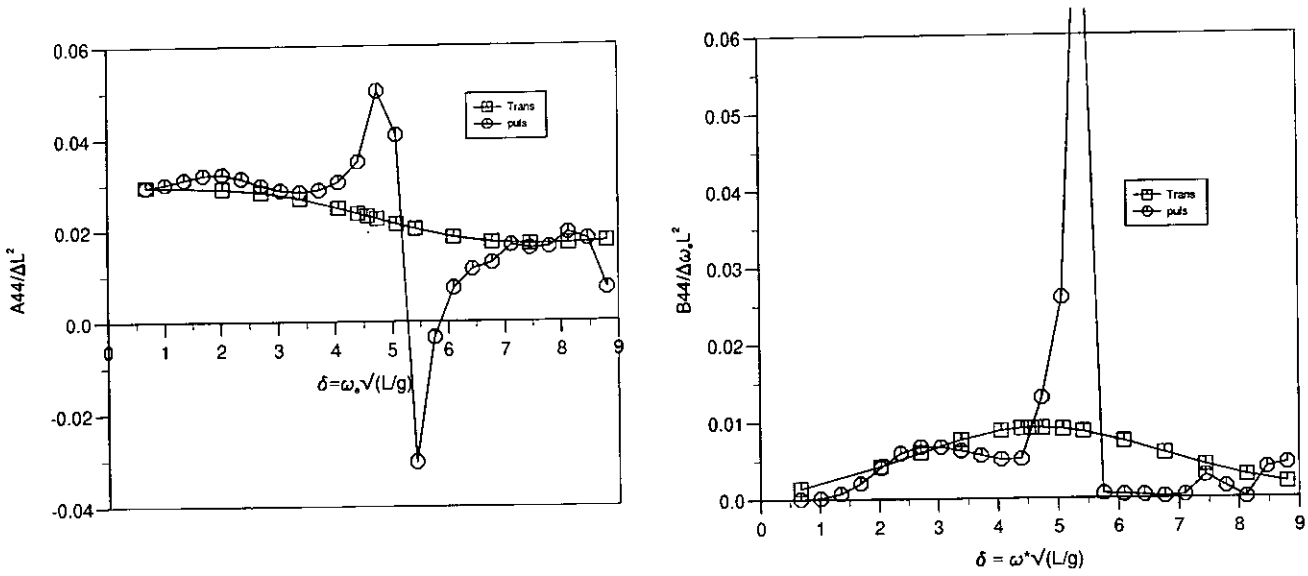

Figure 6: Roll added mass and damping coefficients for model 5s, S/L=0.2, Fn=0.65.

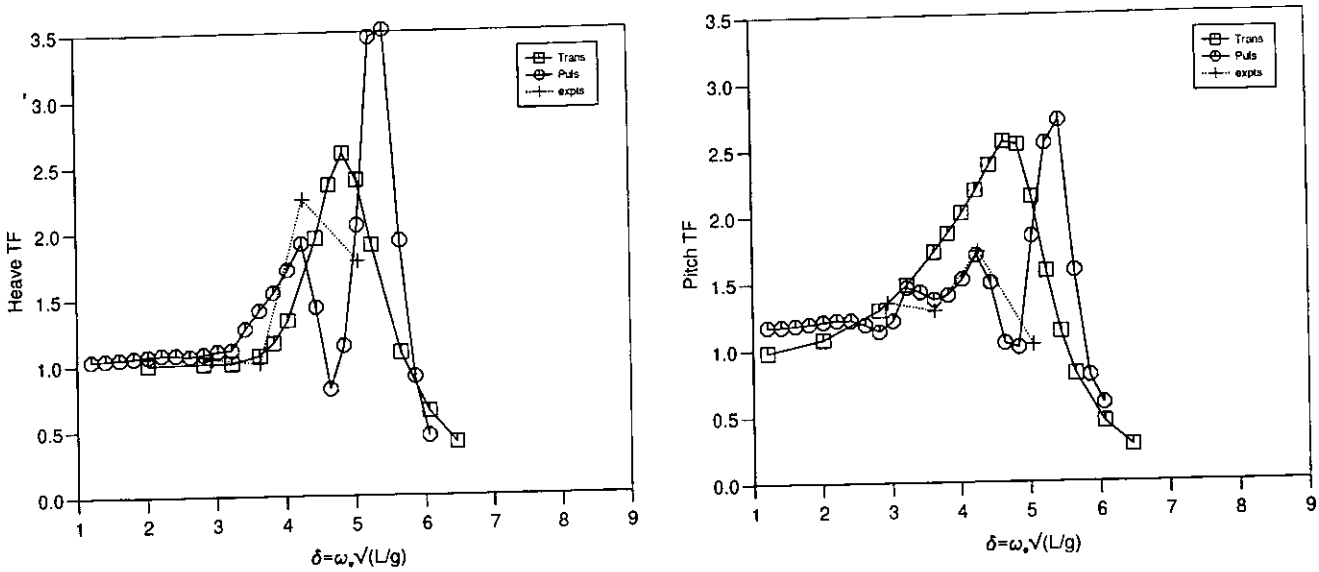

Figure 7: Heave and Pitch Transfer Functions for Model 5b, S/L=0.40 at Fn=0.65, $\chi = 180°$.

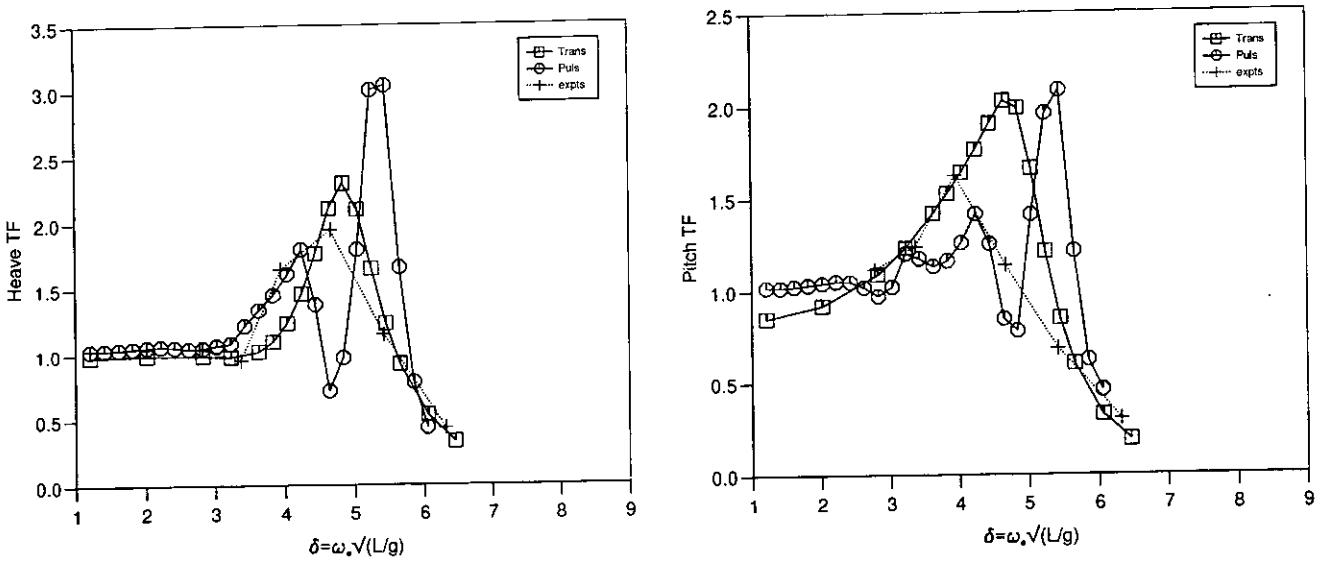

Figure 8: Heave and Pitch Transfer Functions for Model 5b, S/L=0.40 at Fn=0.65, $\chi = 150°$.

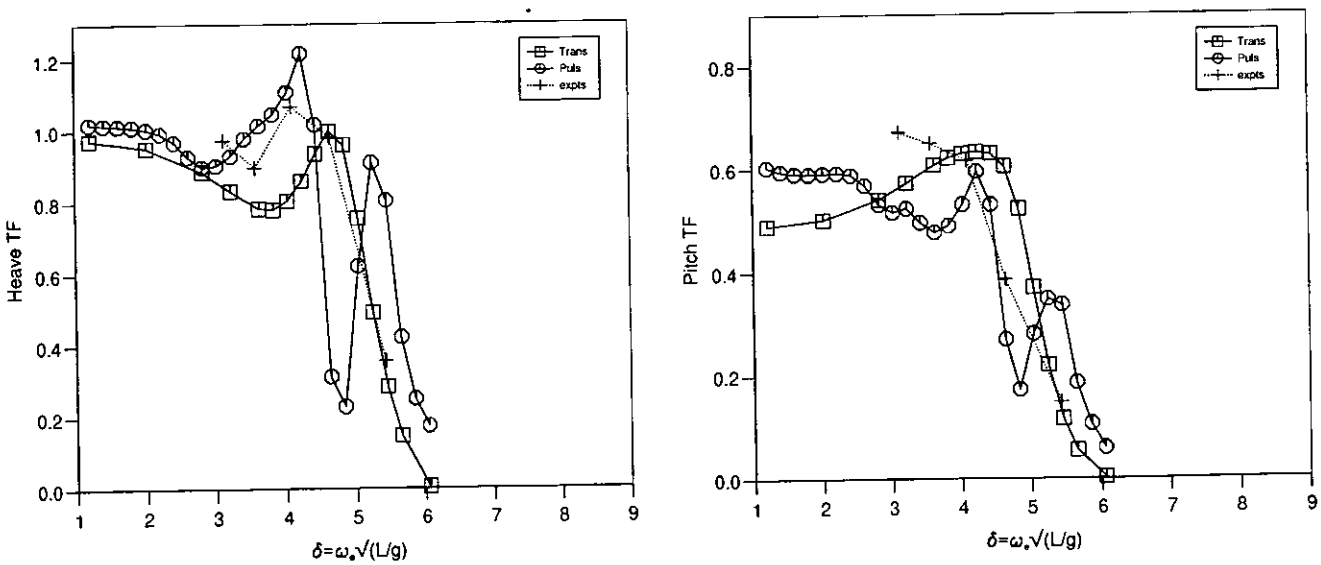

Figure 9: Heave and Pitch Transfer Functions for Model 5b, S/L=0.40 at Fn=0.65, $\chi = 120°$.

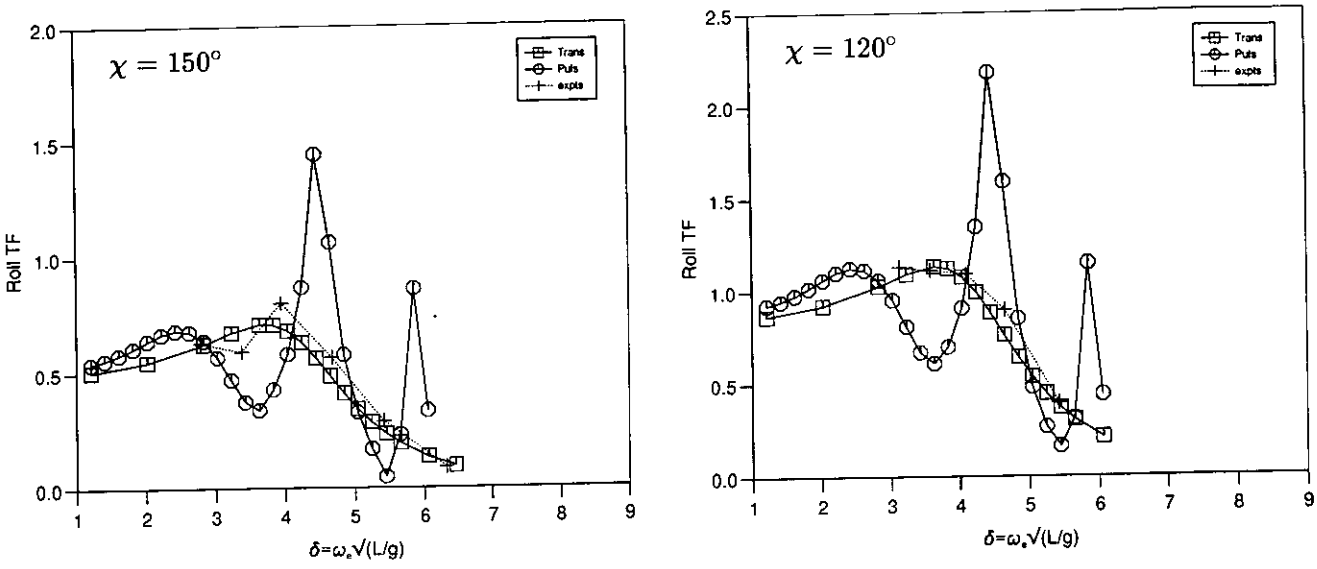

Figure 10: Roll Transfer Functions for Model 5b, S/L=0.40 at Fn=0.65, $\chi = 150°$ and $\chi = 120°$.

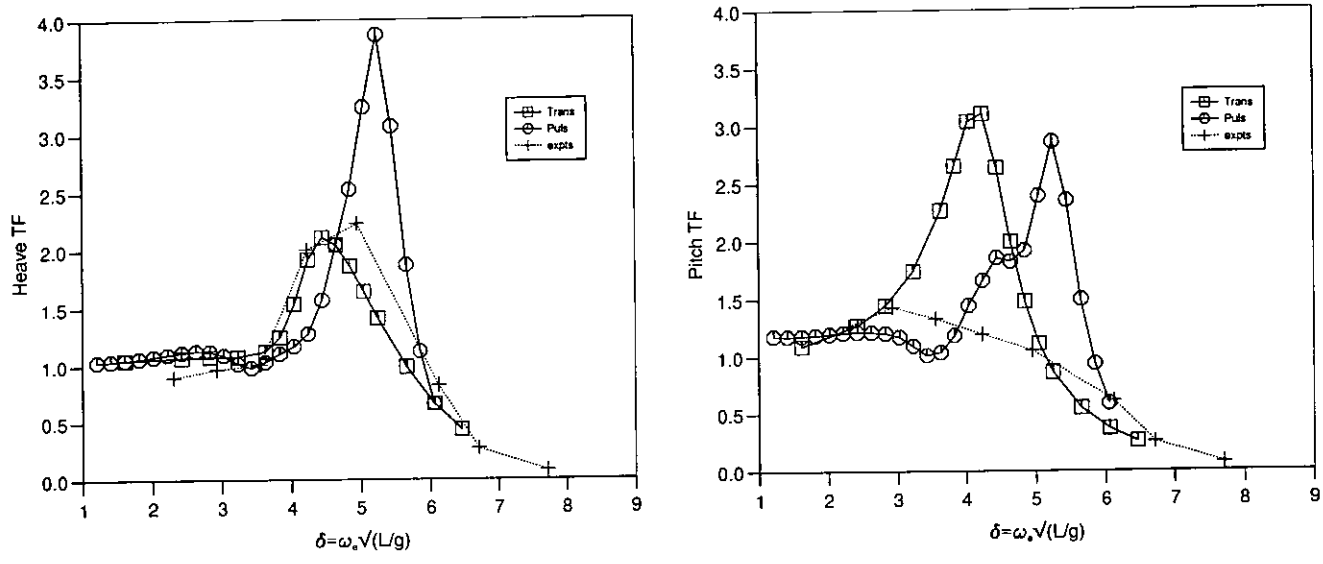

Figure 11: Heave and Pitch Transfer Functions for Model 5b, S/L=0.20 at Fn=0.65, $\chi = 180°$.

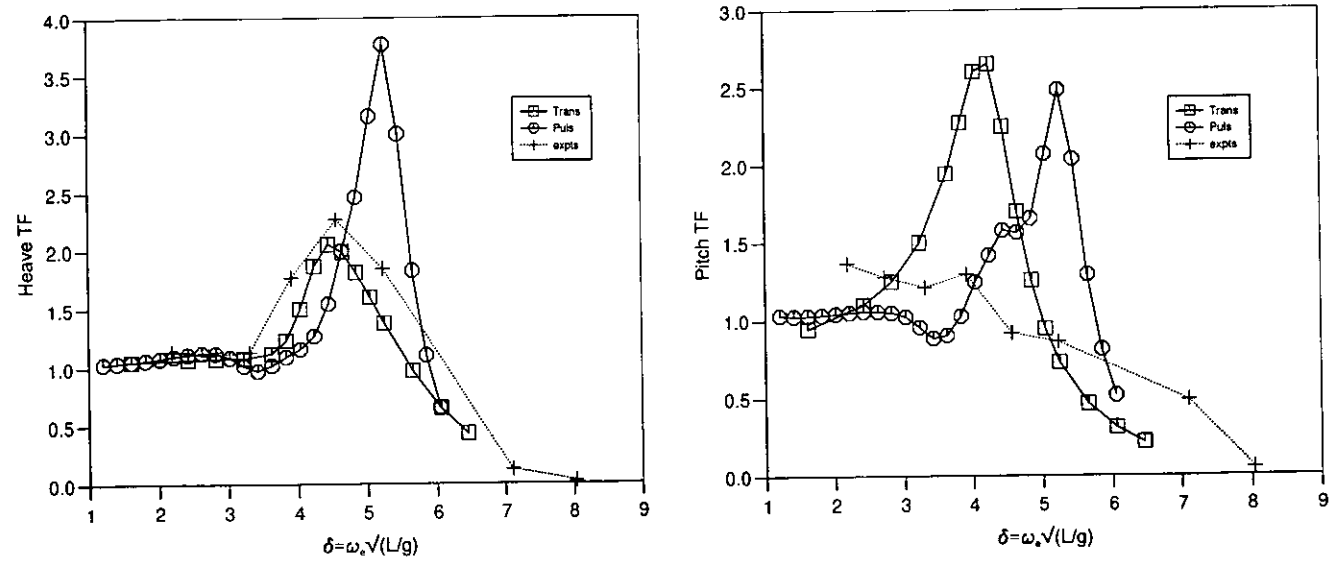

Figure 12: Heave and Pitch Transfer Functions for Model 5b, S/L=0.20 at Fn=0.65, $\chi = 150°$.

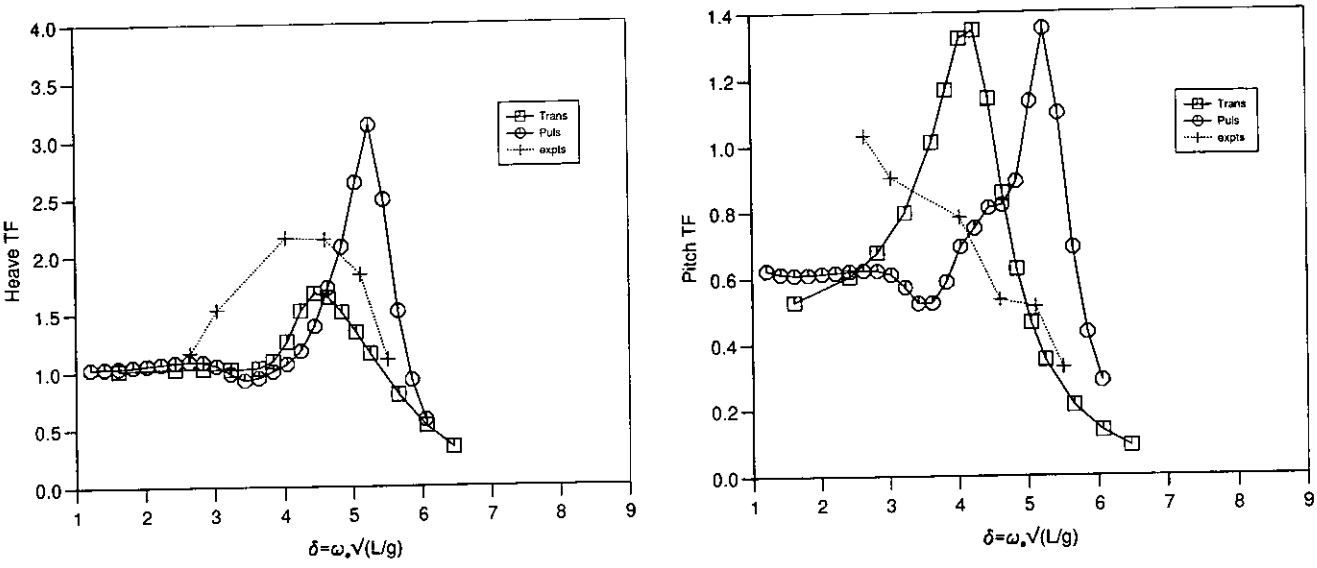

Figure 13: Heave and Pitch Transfer Functions for Model 5b, S/L=0.20 at Fn=0.65, $\chi = 120°$.

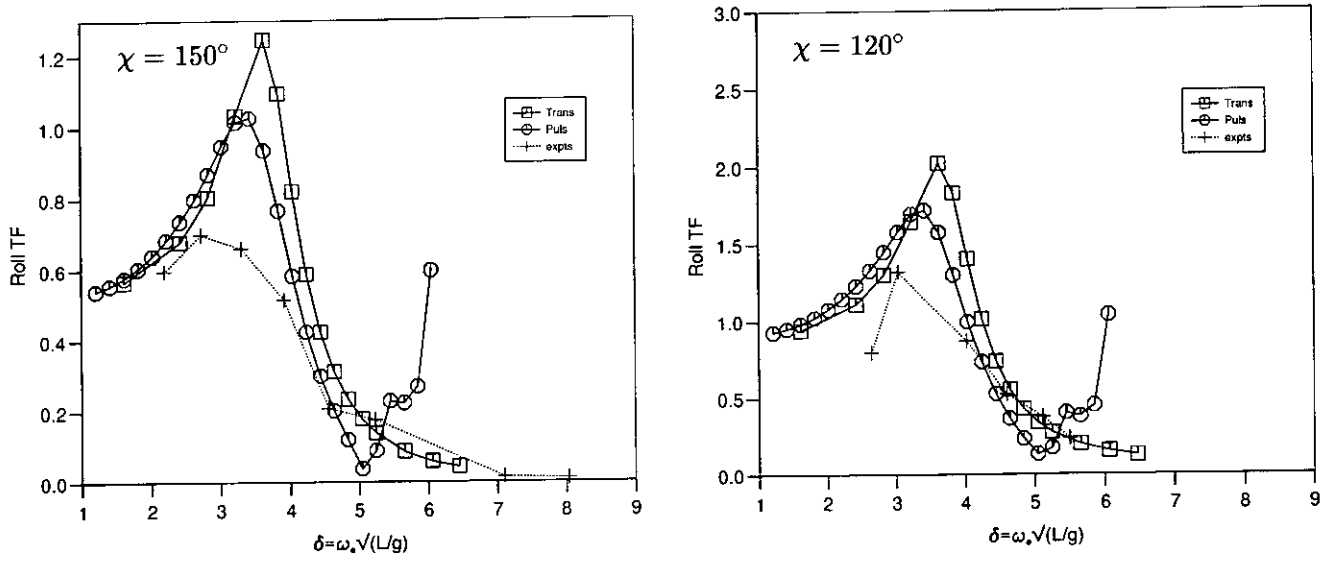

Figure 14: Roll Transfer Functions for Model 5b, S/L=0.20 at Fn=0.65, $\chi = 150°$ and $\chi = 120°$.

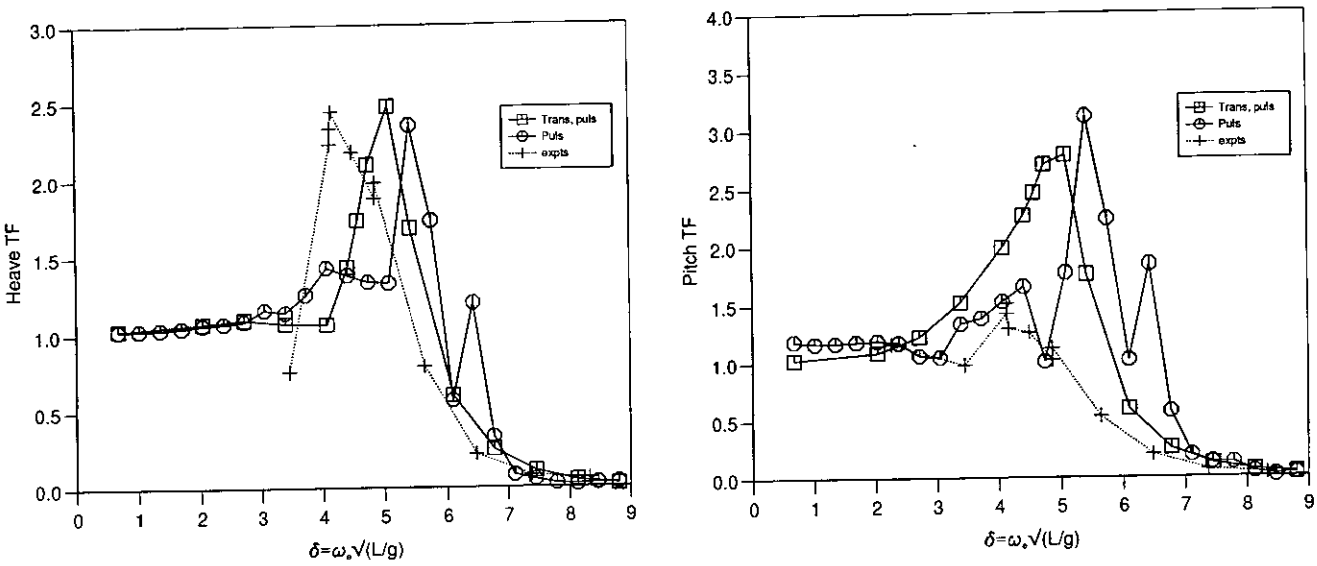

Figure 15: Heave and Pitch Transfer Functions for Model 5s, S/L=0.40 at Fn=0.65, $\chi = 180°$.

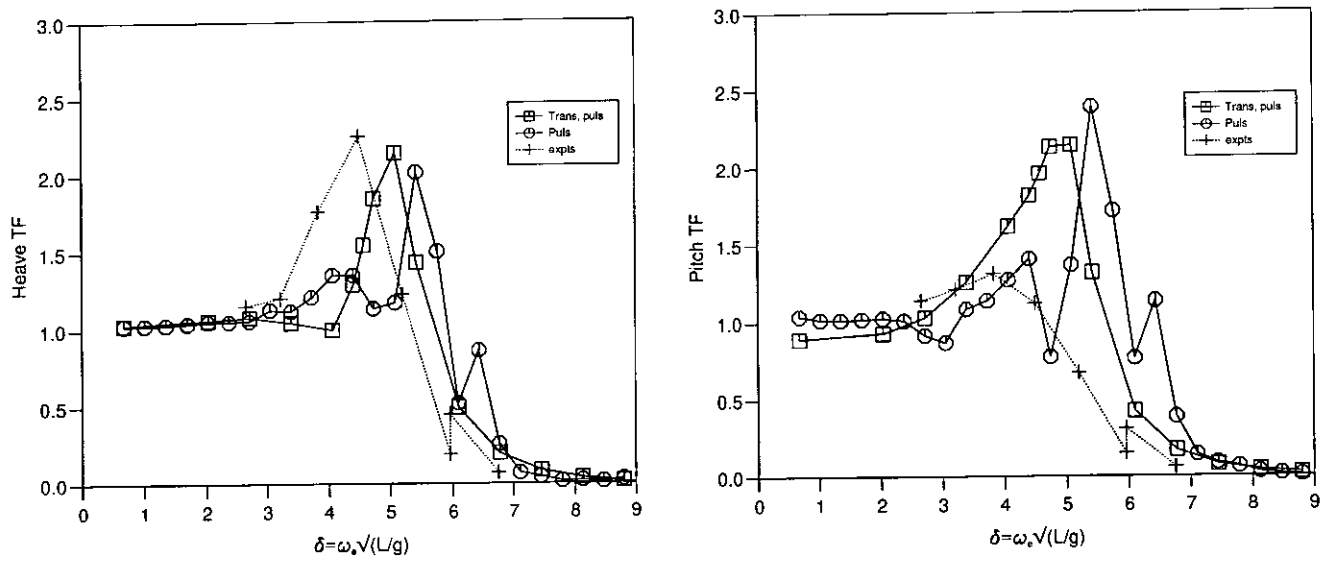

Figure 16: Heave and Pitch Transfer Functions for Model 5s, S/L=0.40 at Fn=0.65, $\chi = 150°$.

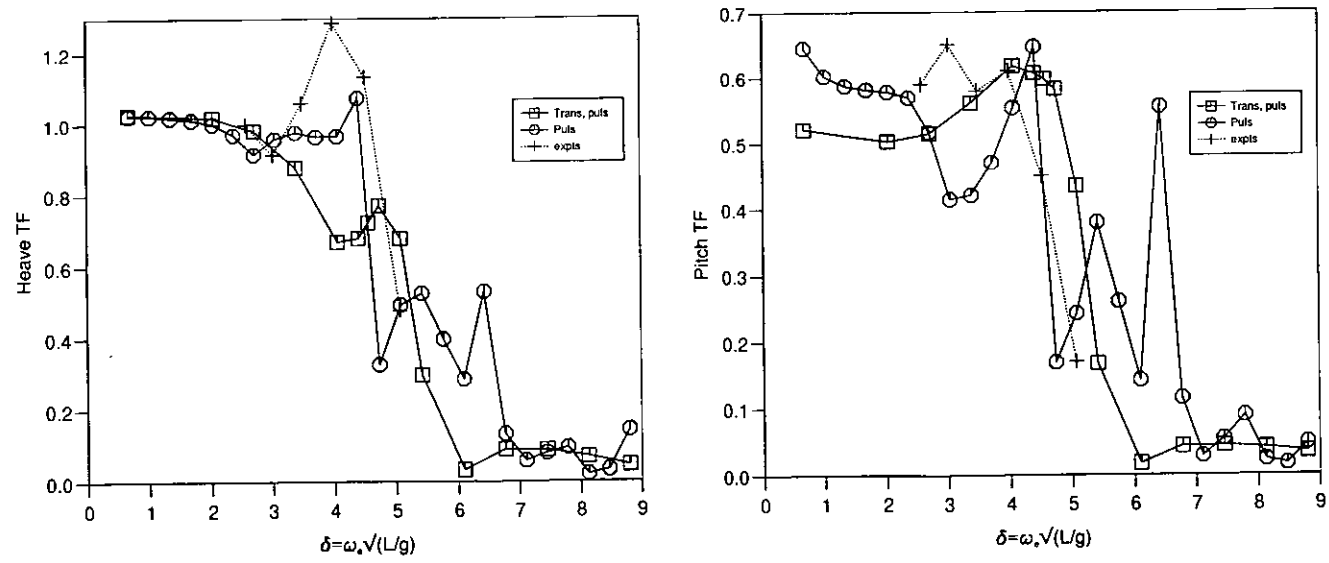

Figure 17: Heave and Pitch Transfer Functions for Model 5s, S/L=0.40 at Fn=0.65, $\chi = 120°$.

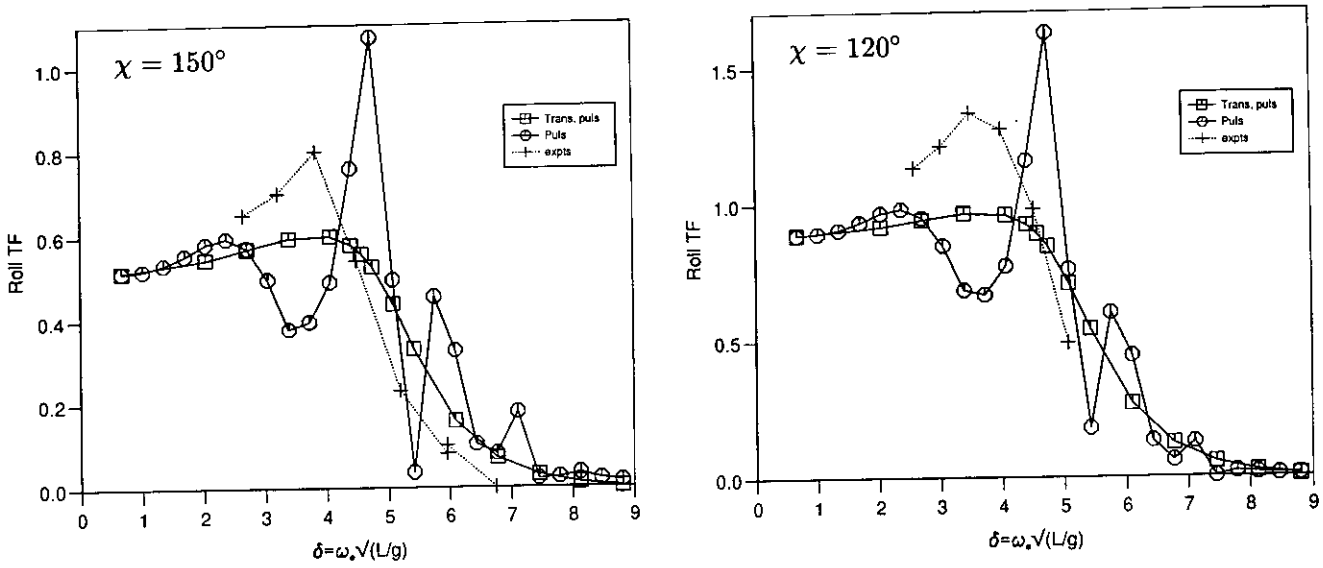

Figure 18: Roll Transfer Functions for Model 5s, S/L=0.40 at Fn=0.65, $\chi = 150°$ and $\chi = 120°$.

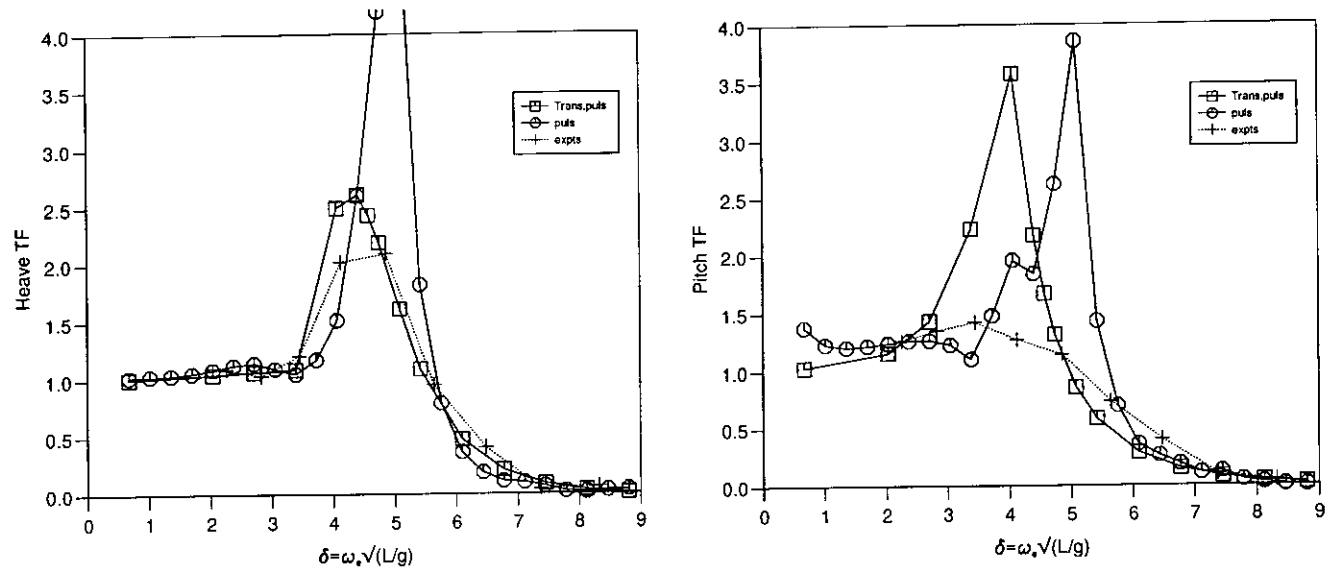

Figure 19: Heave and Pitch Transfer Functions for Model 5s, S/L=0.20 at Fn=0.65, $\chi = 180°$.

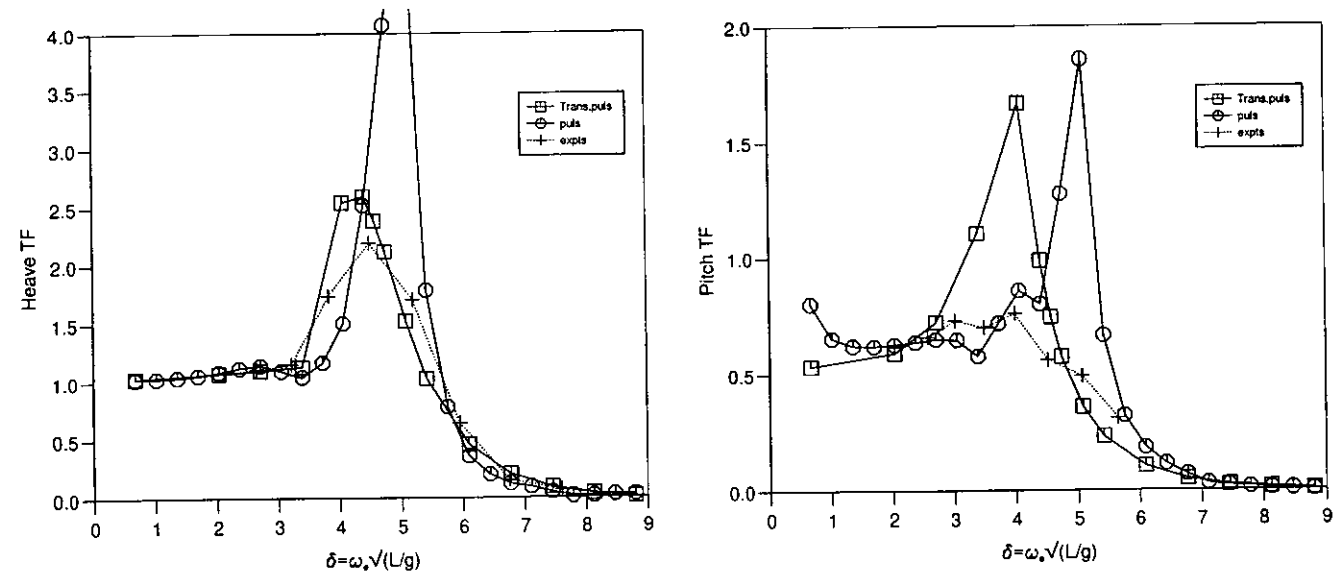

Figure 20: Heave and Pitch Transfer Functions for Model 5s, S/L=0.20 at Fn=0.65, $\chi = 150°$.

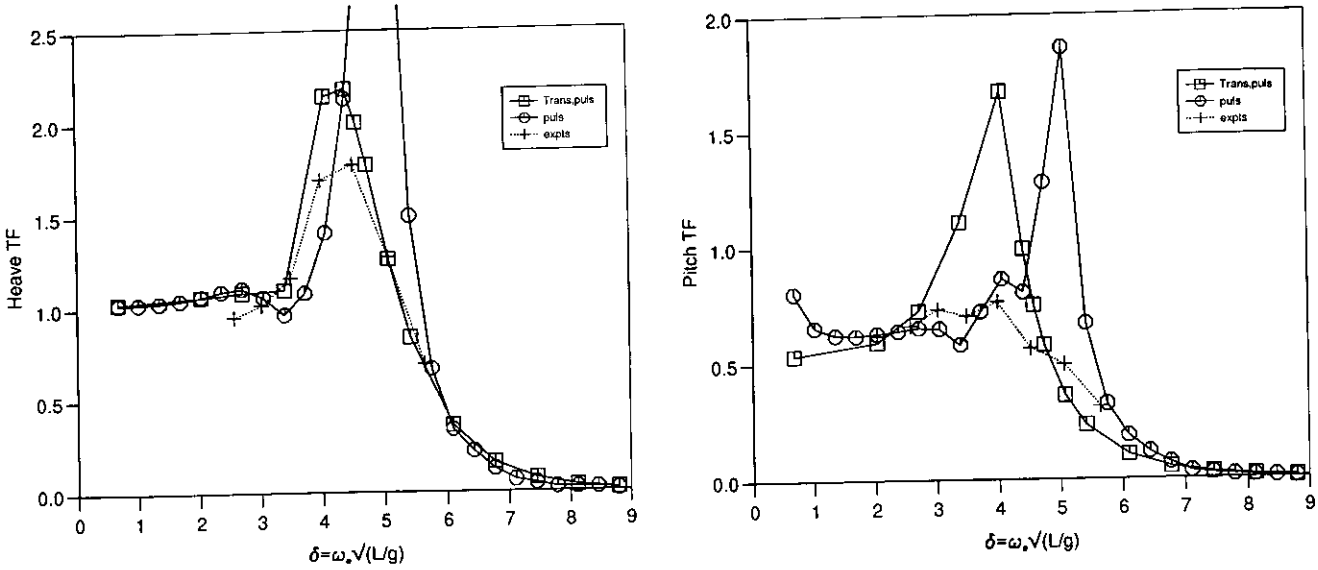

Figure 21: Heave and Pitch Transfer Functions for Model 5s, S/L=0.20 at Fn=0.65, $\chi = 120°$.

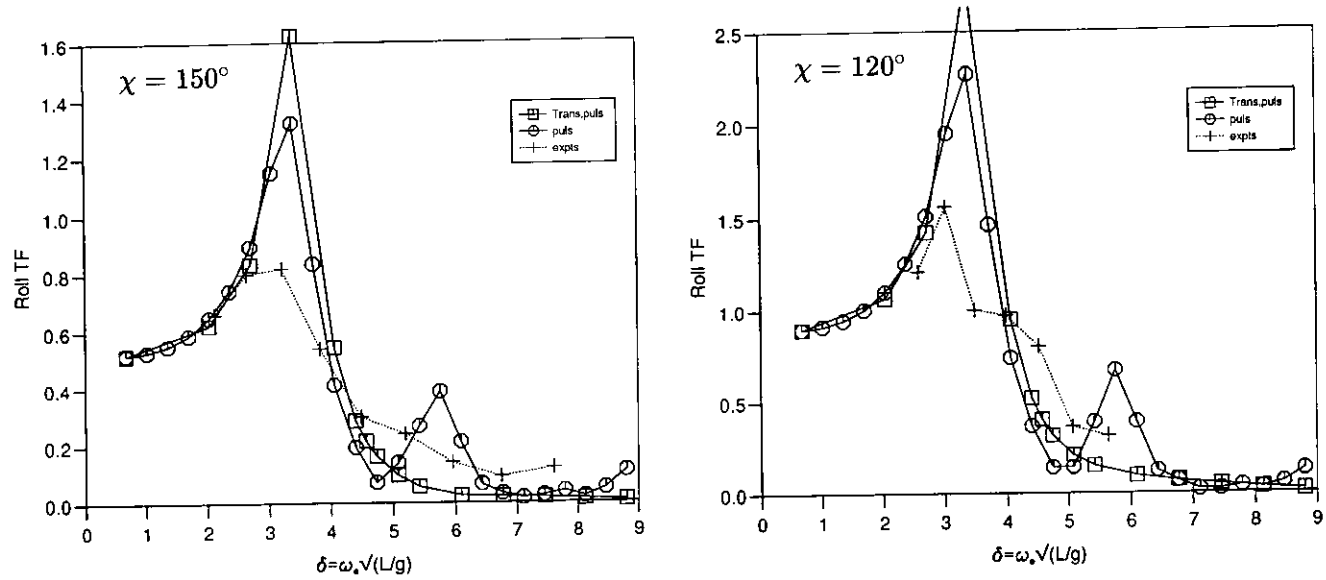

Figure 22: Roll Transfer Functions for Model 5s, S/L=0.20 at Fn=0.65, $\chi = 150°$ and $\chi = 120°$.

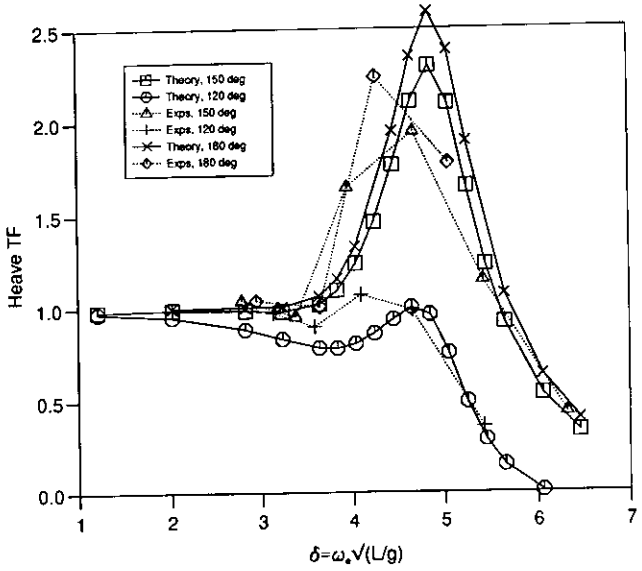

Figure 23: Heave Transfer Functions for Model 5b, S/L=0.40 at Fn=0.65.

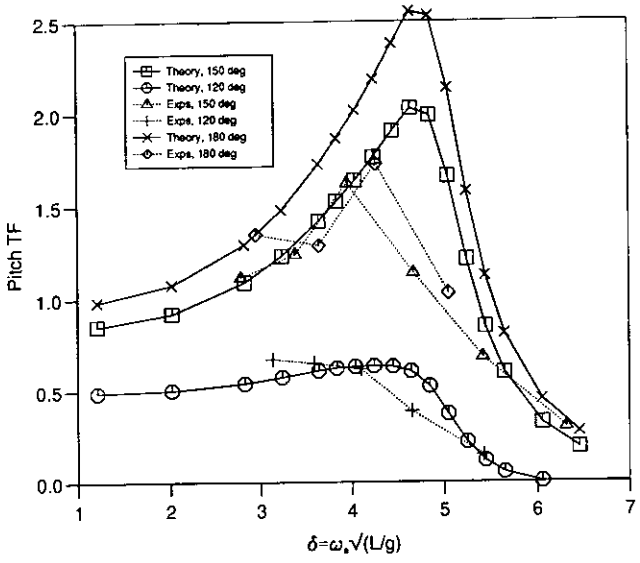

Figure 24: Pitch Transfer Functions for Model 5b, S/L=0.40 at Fn=0.65.

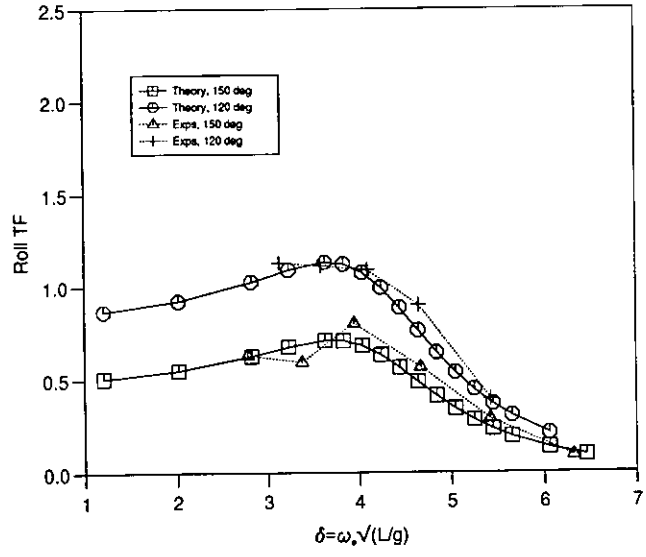

Figure 25: Roll Transfer Functions for Model 5b, S/L=0.40 at Fn=0.65.

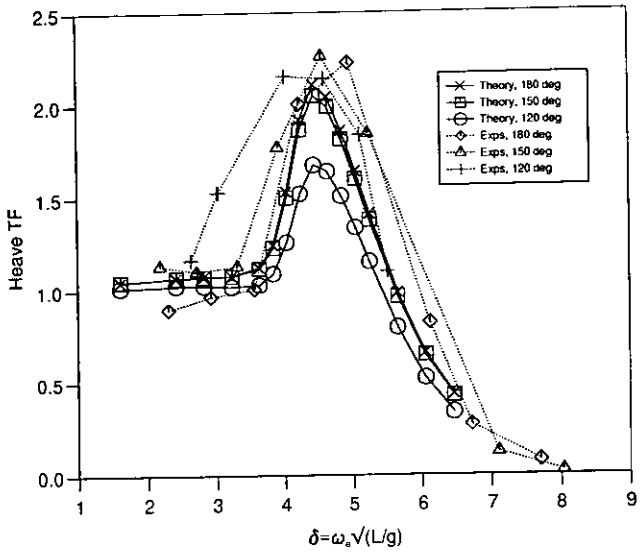

Figure 26: Heave Transfer Functions for Model 5b, S/L=0.20 at Fn=0.65.

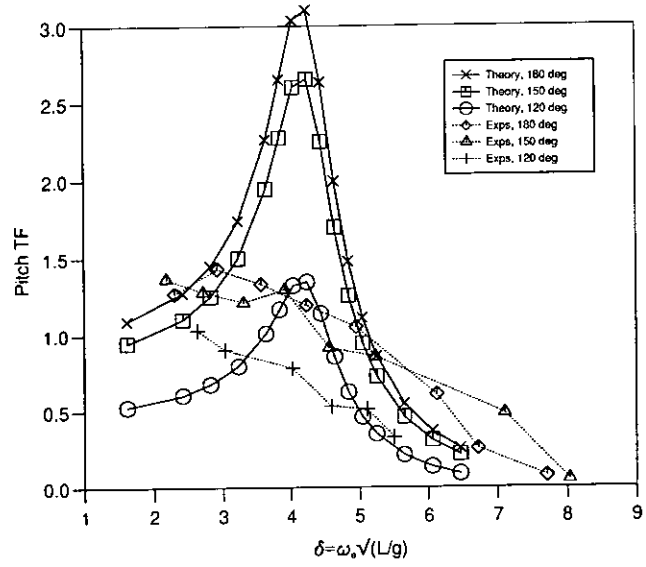

Figure 27: Pitch Transfer Functions for Model 5b, S/L=0.20 at Fn=0.65.

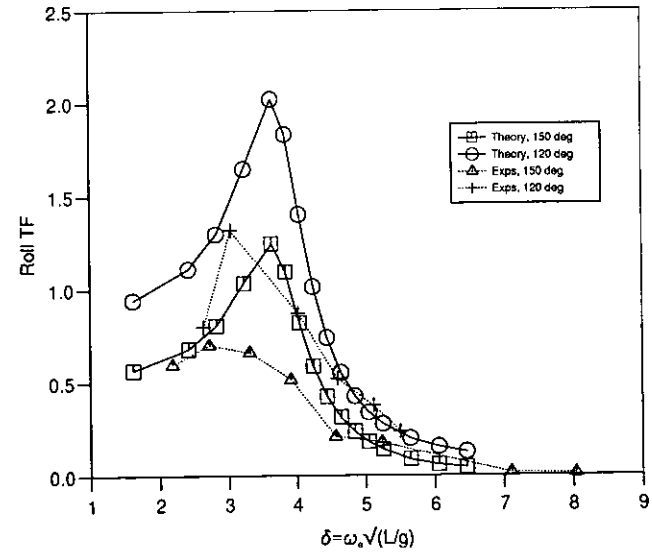

Figure 28: Roll Transfer Functions for Model 5b, S/L=0.20 at Fn=0.65.

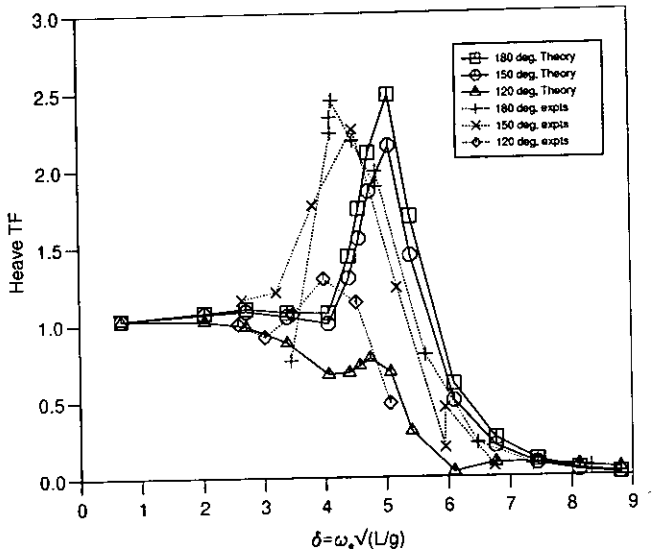

Figure 29: Heave Transfer Functions for Model 5s, S/L=0.40 at Fn=0.65.

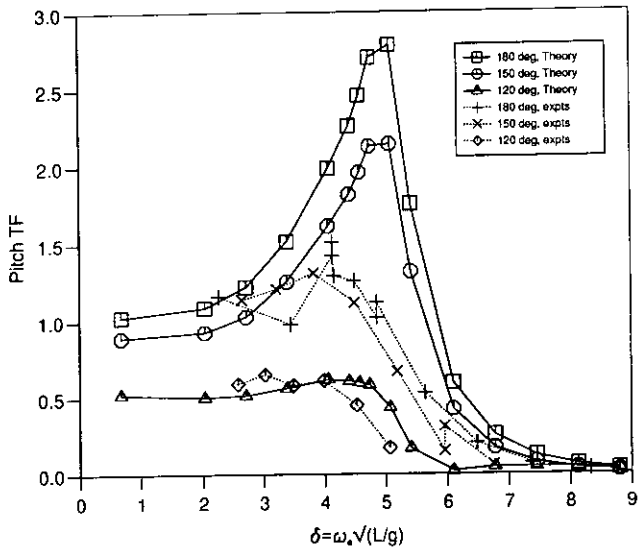

Figure 30: Pitch Transfer Functions for Model 5s, S/L=0.40 at Fn=0.65.

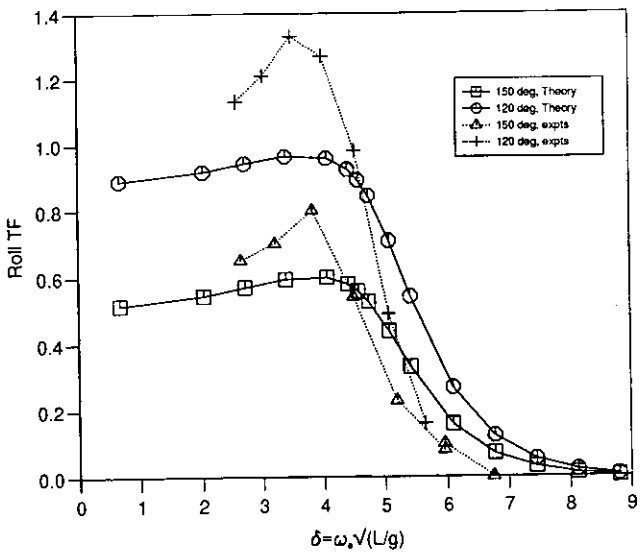

Figure 31: Roll Transfer Functions for Model 5s, S/L=0.40 at Fn=0.65.

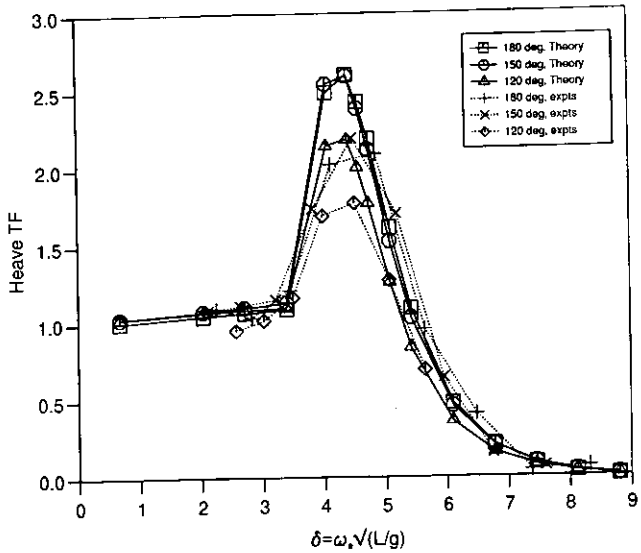

Figure 32: Heave Transfer Functions for Model 5s, S/L=0.20 at Fn=0.65.

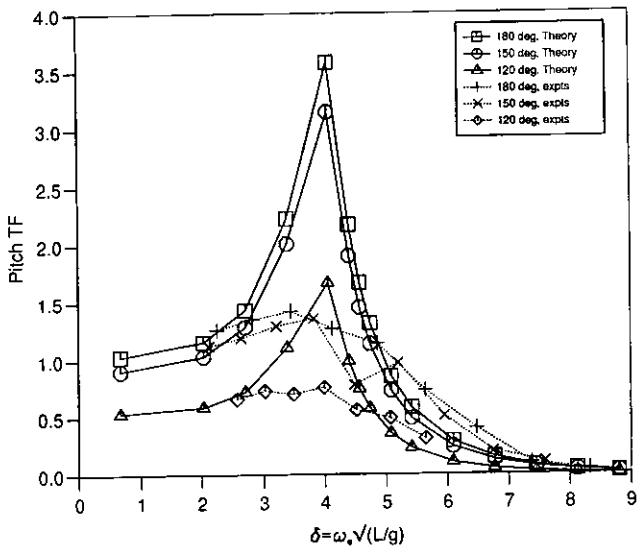

Figure 33: Pitch Transfer Functions for Model 5s, S/L=0.20 at Fn=0.65.

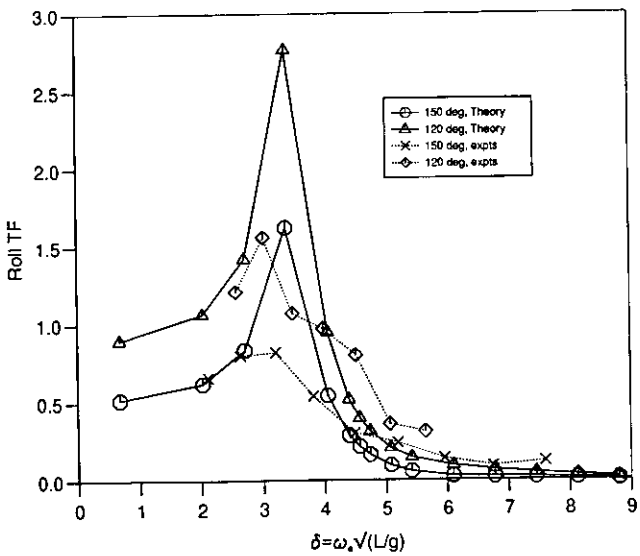

Figure 34: Roll Transfer Functions for Model 5s, S/L=0.20 at Fn=0.65.